Surface Plasmon Grating Coupled Emission from Organic Emitter for Detecting Refractive Index Variation

Nan-Fu Chiu*, Jiun-Haw Lee** and Chii-Wann Lin***

* Institute of Electro-Optical Science and Technology, National Taiwan Normal University, No. 88, Sec. 4, Ting-Chou Road, Taipei, 11677 Taiwan, nfchiu@ntnu.edu.tw
** Department of Electrical Engineering, Graduate Institute of Photonics and Optoelectronics, National Taiwan University, jhlee@cc.ee.ntu.edu.tw
*** Department of Electrical Engineering, Institute of Biomedical Engineering, National Taiwan University, cwlinx@edu.tw

ABSTRACT

We demonstrated the surface plasmon grating coupled emission (SPGCE) from photo-excited organic layer covered with metal thin film on the corrugated substrate. Directional emissions corresponded to the resonant condition of surface plasmon modes on the Au/air interface. In our experiments, we used different pitch sizes to control plasmonic band-gap which produced highly directional SPGCE with enhanced intensity. Based on our calculation, SPGCE showed a color change from yellowish green to orange at a certain viewing angle, while the concentration of contacting glucose was increased from 10 to 40%, corresponding to the refractive index change from 1.3484 to 1.3968. This indicated a potential application of low-cost, integrated, and disposable refractive-index sensor.

Keywords: surface plasmon grating coupled emission (SPGCE), directional, plasmonic band-gap, refractive-index sensor

1 INTRODUCTION

Surface plasmon polariton (SPP) is a kind of longitudinal surface charge density oscillation, which can be resonantly excited at the metal/dielectric interface [1-4]. Recently, enhanced emission of organic emitter on the metallic thin film has been reported by coupling SPPs via energy transfer [5-7]. Such kind of SP coupled emission from fluorescent molecules can be used for biomedical sensing applications [8-12]. In this paper, we used the emission of tris-(8-hydroxyquinoline) aluminum (Alq_3), which was optically pumped by 405 nm semiconductor laser, to excite SPPs on grating structure for surface plasmon (SP) emission. The emissions correspond to the resonant condition of SP modes on the Alq_3/Au interface and grating couple to the Au/air interface for the emission of light, which is called surface plasmon grating coupled emission (SPGCE) [13,14]. This phenomenon gives rise to a viewing-angle-dependent spectral shift, together with the intensity modulation, due to a local field enhancement. This method can be readily extended to detect refractive index changes by using SP coupled fluorophores having different wavelength emissions at different viewing angles. Compared with Kretchmann-Raether configuration, by replacing the electrically pumped organic light-emitting device, together with nano-grating to replace prism, it is possible to reduce the size and price of such a SP sensor for disposable and home-monitoring applications [13,14,15,16]. Besides, in a conventional Kretschmann-Raether configuration, small change in scattered angle was detected due to refractive index difference at a surface with monitoring a single wavelength pumping light. Instead, our approach generated a broadband signal from the pump beam. In this case, one can observe a significant difference in spectral shift at a certain viewing angle which can be clearly distinguished by human eyes without the need of optoelectronic devices such as spectrometer or photodetector [15]. Dynamic range (in terms of refractive index variation, Δn) of such a sensor was as large as 0.128, which was determined by the emission band of the organic emitter.

2 EXPERIMENTS

Fig. 1(a) shows our measurement configuration for detecting photoluminescence (PL) at different viewing angles. Pumping light from a 405 nm diode laser (BWB-405-20E, B&W TEK Inc.) with an incident angle of 45° normal to the surface of the sample, was used to excite the Alq_3 with a broad spontaneous emission band (480 to 680 nm). A spectrometer (USB2000-VIS-NIR, Ocean Optics Co.) mounted on the detector stage was rotated to collect the SPCGE signals at different viewing angles scattered from the corrugated thin film structures. Fig 1(b) shows the detailed cross section of our device structures. Upon the Si-substrate, the photoresist (PR) 1-D grating with 400, 500, 600 and 800 nm was fabricated by Electron-Beam Lithography system (ELS-7500EX, ELIONIX Co.) first, following the deposition of Alq_3 and Au layer, which results in the corrugated structure of Alq_3 and Au thin films. Detailed fabrication processes can be found in Refs. 13 and 14. Dielectric materials (such as, in vitro diagnostics and drug screening for biomedical applications) are in contact with the top side of the Au layer, which may result in a different spectral response of the SPGCE in our calculation results shown below. Fig. 1(c) and its inset show the SEM and AFM pictures of the samples with the structure of Alq_3 (80 nm)/Au (40 nm) on the silicon substrate, respectively.

The photoresist thickness is 100 nm on the silicon substrate with an exposure area of 1.2×1.2 mm^2.

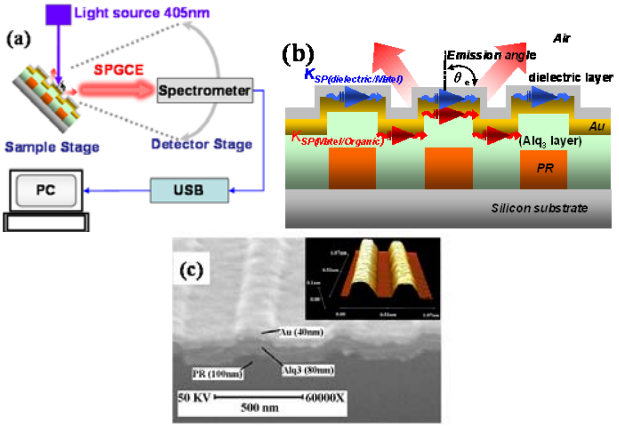

FIG. 1. (a) Experimental setup of the measurement system, (b) schematic diagram of the device cross-section, and (c) SEM and AFM (inset) images of the sample with grating pitch 500 nm.

3 RESULTS AND DISCUSSIONS

3.1 Directional PL emission due to SPGCE

Fig. 2(a) shows the 3-D plot of PL spectra at different viewing angles of the sample with pitch= 500 nm. In this measurement, spectra were taken every 1 degree. Strongest emission occurred at -28° with the wavelength of 620 nm, which was 10.38 times higher than that of PL peak intensity of planar Alq_3 (peak at 546 nm, with full width at half maximum of 100 nm). Besides, the emission angle ranged from -10 to -35° covering the visible spectrum from 500 to 700 nm. With the increasing viewing angle (in absolute value), a red shift was observed corresponding to a color change from greenish blue to red from -10 to -35°. These results suggested a highly directional SPGCE with enhanced light extraction efficiency. Excitons in organic emitters transferred their energy to SP mode at the metal/organic emitter interface [17,18]. Typically, SPs cannot radiate out in a planar OLED structure and is regarded as a quenching term because the wavevector matching condition is not satisfied. With the introduction of corrugated structure, which provides an additional in-plane wave vector, wavevector matching condition of in-plane wave vector ($k_{//}$) and SP wave vector (k_{sp}) in one-dimensional nanostructures can be obtained. There are two possible SPs, i.e. $k_{sp(Au/air)}$ and $k_{sp(Au/Alq3)}$, which can be expressed as:

$$k_{//} = k_{Alq3}\sin\theta = \frac{\omega}{c}\sqrt{\frac{\varepsilon_{Alq3}\varepsilon_m}{\varepsilon_{Alq3}+\varepsilon_m}} \pm m\frac{2\pi}{\Lambda} = k_{sp(Au/Alq3)} \quad (1)$$

$$k_{//} = k_0\sin\theta = \frac{\omega}{c}\sqrt{\frac{\varepsilon_m}{1+\varepsilon_m}} \pm m\frac{2\pi}{\Lambda} = k_{sp(Au/air)} \quad (2)$$

where k_{Alq3} and k_0 are the wave vectors in organic material and air, respectively. θ represents the incident angle. c, ε_{Alq3}, ε_m are light velocity, relative permittivity of dielectric (organic emitters) and metal. m is an integer, and is the grating pitch, respectively [18]. ε_{Alq} is wavelength dependent, which is a complex value with the real and imaginary parts of 2.979 and 0.0124, respectively, at the PL peak of the planar Alq_3 (546 nm). Intensities of these two SPs (metal/air and metal/organic) were strongly dependent on device geometries and structures [17]. In our device, although there are two possible SPR modes, i.e. Alq_3/Au and Au/air, only Au/air signal was observed experimentally [13,14,17,18]. When reducing Au thicknesses from 40 to 20 nm, both metal/air and metal/organic SPs can be observed (results not shown here). That means metal/Alq_3 SPR can be impeded by Au thin film. In our application as biosensor, we would like to increase the intensity of Au/air (Au/dielectric) mode and suppress Au/Alq_3 mode. Hence, we choose a thicker Au (40 nm). Fig. 2(b) shows the spectral peak at different viewing angles with various grating pitches of 400, 500, 600, and 800 nm. One can see a highly directional coupling emission. With the decreasing grating pitch, grating diffraction term ($2\pi/\Lambda$) in Eqs. 1 and 2 increases, which results in a larger diffraction angle (in absolute value).

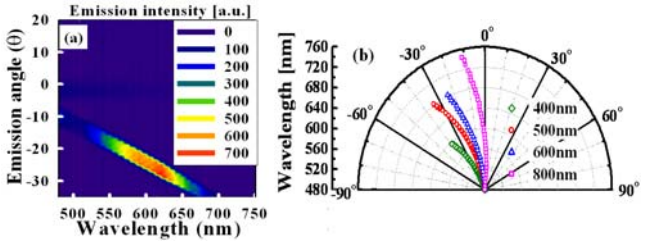

FIG. 2. (a) 3-D plot of PL spectra at different viewing angles of the device (grating pitch=500 nm), and (b) spectral peaks at different viewing angles for the devices with different pitches.

From the measured data of four different pitch samples, we can use peak emission wavelength at each emission angle to calculate its dispersion curve (ω-k relation) by Eq. (2), as shown in Fig. 3. Closed symbols represent the measured ω-k relations extracted from Fig. 2(b), which fall within the light cone defined by the two black dashed lines in Fig.3. That means the wavevector matching conditions can be matched which results in an efficient emission from the SPR mode to the air, corresponding to m= -1 case from Eq. 2. Open symbols shows the calculation results when adding the momentum terms ($2\pi/\Lambda$) for different pitches, corresponding to m=0. In this case the ω-k relation is independent to the grating pitch. With the decreasing grating pitch, grating diffraction term ($2\pi/\Lambda$) in Eq. 2 increases, which results in a larger shift in momentum space from m= 0. Table I summarized the range of emission angle (θ_e) and peak emission angle (MPθ_e) of SPCGE with different pitches experimentally, together with the

calculation results of momentum shift (ΔK). Although some of the grating periods (ex: 600 and 800 nm) were bigger than the emission band of Alq_3 (480-680 nm), however, according to Eq. 2, grating was used to provide an extra in-plane wacevector for satisfying wavevector matching condition. As shown in Fig. 3, 800 nm grating indeed provided enough wavevector displacement for detecting SP signals.

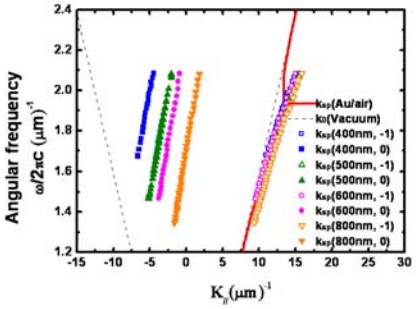

FIG. 3. Dispersion relations (ω-k). Solid symbols show the experimental data (m=-1) with different grating pitches. Open symbols are the the calculated results corresponding to m=0. Solid and dashed lines represent calculation results of dispersion relation at Au/air interface and that in the air, respectively.

TABLE 1: Range of SPCGE emission angle (θ_e), emission angle with maximum emission intensity (MPθ_e), and momentum shift (△K) with different pitches.

Pitch(nm)	(θ_e)	(MP θ_e)	△K(μm)$^{-1}$
400	-40° ~ -30°	-37°	18.98234
500	-35° ~ -10°	-28°	16.74774
600	-25° ~ -5°	-15°	14.43099
800	-10° ~ 10°	0°	13.52638

(θ_e) is emission angle.
(MP θ_e) is Max peak of emission angle.

3.2 SPGCE for sensor application

For sensor application, materials with different dielectric constants (ε_d) can be introduced upon the Au layer of the device, which corresponds to materials with different refractive index. Here, Eq. 2 should be modified as follows

$$k_{//} = k_d \sin\theta = \frac{\omega}{c}\sqrt{\frac{\varepsilon_d \varepsilon_m}{\varepsilon_d + \varepsilon_m}} \pm m\frac{2\pi}{\Lambda} = k_{sp(Au/dielectric)} \quad (3)$$

where kd is wave vector and d is relative permittivity of dielectric material. When ε_d =1, it corresponds to the air and converges to Eq. 2. However, it is not easy to realize such a device (dielectric on thin Au) experimentally in this stage. When dielectric (such as solution) contacted the thin metal film, it easily penetrated the Au, attack Alq_3, and degrade PL intensity [19]. To improve, suitable passivation thin film should be adopted to protect the devices [20]. In our calculation, grating pitch is set at 500 nm. ε_m values of Au at different wavelengths can be found in Ref. 21. Here, ε_d of water is 1.772 and that of glucose with 10, 20, and 40% are 1.818, 1.862, and 1.951, respectively in our calculation [22]. Fig. 4(a) shows the calculation results from Eq. 3 and parameters given above, with the increasing value of ε_d, one can see a right shift of the ω-k curves, which corresponds to an increase in momentum space. Sensitivity of this device can be calculated based on following equation [23]:

$$\sigma_n = \frac{\Delta n}{\Delta\lambda}\sigma_\lambda \quad (4)$$

Here, σ_n is the resolution in terms of RIU. Δn and Δλ are the refractive index difference and corresponding wavelengths change, respectively. σ_λ is the wavelength resolution of the spectrometer. Based on the Δn and Δλ values of glucose 10% and 20% measured the angle 1o, sensitivity in our measurement system is:

$$\sigma_n = \frac{\Delta n}{\Delta\lambda}\sigma_\lambda = \frac{1.3644 - 1.3484}{604.83 - 576.28} \times 0.3 \quad (5)$$
$$= 5.604 \times 10^{-4}\ RIU/nm \times 0.3nm = 1.681 \times 10^{-4}\ \text{RIU}$$

This RIU value is not as high as other SPR sensors (ex: 5×10^{-7} RIU in Ref. 23). However, it is good enough as a biosensor for detecting some large molecules, such as diagnosis of tuberculosis in blood serum, with specific binding technique on the surface of the biosensor, which required a refractive index change of 2.2×10^{-4} [24]. Note that in this setup, the resolution of the spectrometer is 0.3 nm with the physical size small and portable. By using high resolution spectrometer (σ_λ=0.01), the sensitivity can be improved to 5.604×10^{-6} [25].

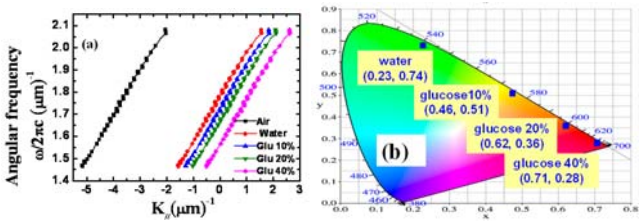

FIG. 4. (a) Calculated dispersion relation with different species contacting the top side of the sample, and (b) calculated CIE coordinates shift with a fixed viewing angle with different species.

Fig. 4(b) shows the CIE coordinates in chromaticity diagram with different dielectric materials observed at -13°. One can note that the color changes from green (water), yellow (glucose 10%), orange (glucose 20%), to red (glucose 40%) with the increasing ε_d. Our device emits light with different spectra at visible range when contacting species with different relative permittivities. That means signal detection can be achieved by human eyes at a certain viewing angle without spectrometer. By attaching an optical film to limit the viewing angle, such a device can be used for disposable and point-of-care biosensors with simple

instructions. Wavelength discrimination of human eye is about 2 nm in visible range [26], it yields a sensitivity of:

$$\sigma_n = \frac{\Delta n}{\Delta \lambda}\sigma_\lambda = \frac{1.3644 - 1.3484}{604.83 - 576.28} \times 2 \quad (6)$$
$$= 5.604 \times 10^{-4}\ {}^{RIU}\!/_{nm} \times 2nm = 1.121 \times 10^{-3}\ \text{RIU}$$

This RIU value is quite low. Hence, when using naked eye as the detector, maybe it is not suitable for detecting refractive index change of thin film, such as hybridization-adsorption biosensor with high specificity with small refractive index change [27]. Instead, it can be used for detecting refractive index change in liquid, such as determining protein and glucose concentrations in urine and serum, and fat concentrations in milk and hydroxyl content in soybean oil, with Δn at 10^{-3} range [28,29,30].

Besides, our sensor exhibits two possible advantages, which are simple system configuration and large dynamic range. Compared with conventional Kretschmann-Raether configuration, the function of our light source is to pump organic emitter, hence careful optical alignment is not necessary. Provided that electroluminescence can replace optical pump, then the light source can be totally removed in our system. So the optical detection system could be further simplified. Besides, we can also note that the dynamic range of the sensor, in terms of refractive index variation, is large. In visible range, it can be as large as 0.128, which is limited by the emission band of the organic emitter. By employing multiple emitters and extending into infrared region, the dynamic range can be further increased [31,32].

4 SUMMARY

In summary, we demonstrated a highly directional SPCGE with different grating pitches, which comes from the Au/air SP radiation. Based on a simple calculation, ω-k relation fit well with the experimental results, which was extracted from the spectral peak of the viewing angle dependent spectra. When contacting with different materials, SPCGE is sensitive to the dielectric constant. Due to the broadband emission from the organic material, one can observe clear color changes at a certain viewing angle with different ε_d. It is suitable for the application of low cost and disposable sensor application.

ACKNOWLEDGEMENTS:

This project is supported in part by National Science and Technology Program in Pharmaceuticals and Biotechnology, National Science Council, Taiwan, R.O.C., NSC 96-2218-E-002-026, NSC 97-2218-E-002-014, NSC 98-2221-E-002-038-MY3, and NSC 99-2218-E-003-002-MY3.

REFERENCES

[1] R. W. Wood, Phil. Mag. 4, 396,1902.
[2] H. Raether, Surface Plasmons on Smooth and Rough Surface and on Gratings (Springer-Verlag), 1988.
[3] A. Otto, Z. Phys. 216, 398,1968.
[4] E. Kretschmann, Z. Phys. 241, 313,1971.
[5] D. Gifford and D. G. Hall, Appl. Phys. Lett. 80, 3679,2002.
[6] S. Wedge and W. L. Barnes, Opt. Exp. 12, 3673,2004.
[7] J. Feng, T. Okamoto, and S. Kawata, Appl. Phys. Lett. 87, 241109, 2005.
[8] I. Pockrand and A. Brillante, Chem. Phys. Lett. 69, 499,1980.
[9] J. R. Lakowicz, J. Malicka, I. Gryczynski, and Z. Gryczynski, Biochem. Biophys. Res. Commun. 307, 435, 2003.
[10] G. Winter and W. L. Barnes, Appl. Phys. Lett. 88, 051109, 2006.
[11] J. Kalkman, C. Strohhofer, B. Gralak, and A. Polman, Appl. Phys. Lett. 83, 30, 2003.
[12] S. A. Maier, P. G. Kik, H. A. Atwater, S. Meltzer, E. Harel, B. E. Koel, and A. A. G. Requicha, Nat. Mater. 2, 229, 2003.
[13] N.-F. Chiu, C.-W. Lin, J.-H. Lee, C.-H. Kuan, K.-C. Wu, and C.-K. Lee, Appl. Phys. Lett. 91, 083114, 2007.
[14] N.-F. Chiu, C. Yu, S.-Y. Nien, J.-H. Lee, C.-H. Kuan, K.-C. Wu, C.-K. Lee, and C.-W. Lin, Opt. Exp. 15, 11608, 2007.
[15] J. Homola, S. S. Yee, and G. Gauglitz, Sensors and Actuators B, 54, 3,1999.
[16] K. Schult, A. Katerkamp, D. Trau, F. Grawe, K. Cammann, and M. Meusel, Anal. Chem. 71, 5430, 1999.
[17] S. Wedge, A. Giannattasio, and W. L. Barnes, Org. Electron. 8, 136, 2007.
[18] S.-Y. Nien, N.-F. Chiu, Y.-H. Ho, J.-H. Lee, C.-W. Lin, K.-C. Wu, C.-K. Lee, J.-R. Lin, M.-K. Wei, and T.-L. Chiu, Appl. Phys. Lett., 94, 013307, 2009.
[19] P. E. Burrows, V. Bulovic, S. R. Forrest, L. S. Sapochak, D. M. McCarty, and M. E. Thompson, Appl. Phys. Lett. 65, 2922, 1994.
[20] S. J. Yun, Y. W. Ko, and J. W. Lim, Appl. Phys. Lett., 85, 4896, 2004.
[21] E. D. Palik, Handbook of Optical Constants of Solids, edited by (Academic, New York, 1985).
[22] C.-W. Lin, K.-P. Chen, C.-N. Hsiao, S. Lin, and C.-K. Lee, Sens. and Actuators B, 113, 169, 2006.
[23] S. G. Nelson, K. S. Johnston, and S. S. Yee, Sens. and Actuators B, 35, 187, 1996.
[24] T. Nagel, E. Ehrentreich-Förster, M. Singh, K. Schmitt, A. Brandenburg, A. Berka, F. F. Bier, Sens. and Actuators B, 129, 934, 2008.
[25] T. Akimoto, S. Sasaki, K. Ikebukuro, and I. Karube, Biosens. Bioelectron. 15, 355, 2000.
[26] G. G. Wyszecki and W. S. Stiles, Color Science- second ed. (Wiley), 1982.
[27] C. E. Jordan, A. G. Frutos, A. J. Thiel, and R. M. Corn, Anal. Chem. 69, 4939, 1997.
[28] Y. Liu, P. Hering, and M. O. Scully, Appl. Phys. B 54, 18, 1992.
[29] A. J. Jääskeläinen, K. E. Peiponen, and J. A. Räty, J. Dairy Sci. 84, 38, 2001.
[30] W. Xie and H. Li, J. Am. Oil Chem. Soc. 83, 869, 2006.
[31] C.-H. Hsiao and J.-H. Lee, J. Appl. Phys. 106, 024503, 2009.
[32] K. R. Choudhury, D. W. Song, and F. So, Org. Electron. 11, 23, 2010.